

## Nonequilibrium effects in the channeling of energetic particles through ultrathin Si/Ge/Si heterostructures: A Monte Carlo study

H.-J. Gossmann

*AT&T Bell Laboratories, Murray Hill, New Jersey 07974*

(Received 22 August 1988)

Nonequilibrium phenomena in the channeling of 1.8-MeV  $\text{He}^+$  in (2–6)-ML-thick (ML, monolayer) pseudomorphic films of Ge on Si(100) capped with 148 ML of crystalline Si are investigated by use of Monte Carlo techniques. The large asymmetry in the channeling angular scans is related to the strain in the ultrathin film and can be used as a sensitive measure of that strain. The two lattice parameters of interest, at the Si/Ge interface and of the strained Ge film, are extracted by comparing experimental results with simulations. The relevant features in the angular scans on which this determination is based are very sharp functions of angle, typically of  $0.25^\circ$  full width at half maximum. Possible systematic errors arising from this, as well as the influence of other experimental parameters such as beam divergence and the thickness of the Si cap, are assessed.

### I. INTRODUCTION

The channeling of energetic particles (typically  $\text{He}^+$  with energies in the MeV range) has become a useful tool for the determination of structure and properties of materials and in particular of thin films.<sup>1</sup> Typically analysis is characterized by the assumption of statistical equilibrium,<sup>2</sup> leading to an analytical expression for the flux distribution of the channeled particles. This provides information on the crystalline perfection via the minimum yield and on the lattice location of impurities via angular scans and flux-peaking effects.

Statistical equilibrium is attained after the incident particles have traveled a distance of the order of a mean free path  $\lambda$ , typically  $\approx 1000 \text{ \AA}$ .<sup>2</sup> For depths smaller than  $\lambda$  the assumption of statistical equilibrium is no longer valid, leading, for example, to oscillations in the backscattered yield as a function of depth.<sup>3</sup> Other manifestations include the asymmetry in  $\langle 110 \rangle$  angular scans performed in a  $\{110\}$  plane of III-V compounds,<sup>4</sup> and planar dechanneling in strained-layer superlattices.<sup>5</sup> Recent advances<sup>6</sup> in molecular-beam epitaxy have made it possible to grow structures where the absence of statistical equilibrium is particularly striking. For example, angular scans of pseudomorphic, strained-layer heterostructures consisting of between 2 and 6 monolayers (ML) of Ge on a Si(100) substrate, capped with  $\approx 150$  ML of Si, show a dramatic asymmetry in the angular scans of the ultrathin Ge layers.<sup>7</sup> A theoretical understanding of the physical properties of these highly strained structures requires knowledge of the structural parameters. In this paper we will investigate, using a Monte Carlo approach, how the nonequilibrium nature of channeling in these structures can be used to determine structural parameters. We will show that the asymmetry in the angular scans is a direct consequence of the strain in the ultrathin films and that it can be used as a sensitive measure of that strain. We will then explore the limits of that approach and the influence of experimental parameters, such as beam divergence and the thickness of the Si cap.

### II. MONTE CARLO SIMULATION OF CHANNELING

The methods for the simulation of channeling phenomena by Monte Carlo methods have been described by Robinson and Oen,<sup>8</sup> Morgan and van Vliet,<sup>9</sup> and Barrett.<sup>10</sup> The basic idea is to simulate an actual experiment by starting projectiles outside a crystal represented by an array of coordinates, and by calculating their trajectories while they penetrate the target. Each collision is treated classically in the binary collision approximation;<sup>11</sup> scattering angles are evaluated using suitable approximations to the scattering integral.<sup>12</sup> The Molière approximation to the Thomas-Fermi potential is employed as potential.<sup>13</sup> Energy losses of the projectiles, due to inelastic or elastic collisions with nuclei or electrons, are neglected. Following trajectories of projectiles through the simulated crystal results in the flux distribution of the channeled particles as a function of depth. The experimentally accessible value of the backscattering yield from a particular atom is proportional to the nuclear encounter probability for that atom, which, in turn, is proportional to the overlap of the flux distribution with the probability function describing the position of that atom. Thermal motion of an atom is approximated by a Gaussian probability distribution centered around its lattice site. Root-mean-square (rms) vibrational amplitudes of  $0.0787 \text{ \AA}$  for Si and  $0.0870 \text{ \AA}$  for Ge were used.<sup>14</sup> Correlations between the vibrating atoms of the target have been shown to exist in theoretical treatments<sup>15</sup> and tend to decrease the nuclear encounter probabilities.<sup>16,17</sup> Correlations decrease rapidly with distance;<sup>16,18</sup> therefore only correlations between next-nearest neighbors along  $\langle 110 \rangle$  rows of atoms were incorporated. Correlation coefficients of 0.240 and 0.258 for Si and Ge, respectively, were calculated from a Debye model.<sup>19</sup> The influence of correlations on the flux distributions and asymmetry parameters discussed below is only small. No attempt was made to change vibrational amplitudes or correlation coefficients due to the strain in the structure. All simu-

lated angular scans were taken around an off-normal  $\langle 110 \rangle$  axis in a  $\{100\}$  plane.

### III. CHANNELING IN ULTRATHIN HETEROSTRUCTURES: RESULTS

The structural parameters of interest for pseudomorphic strained-layer films are the lattice constants perpendicular to the interface between the Si overlayer and the outermost layer of Ge,  $a_1$ , and within the Ge layer itself,  $a_2$ . Knowledge of  $a_1$  and  $a_2$  allows a calculation of the strain field and thus theoretical investigation of the novel electronic and optical properties expected of highly strained structures. Since the structure is pseudomorphic, i.e., the in-plane lattice constants are the same throughout the whole structure and equal to the Si bulk lattice constant,  $a_{\text{Si}} = 5.4307 \text{ \AA}$ , a first reasonable estimate would be to set  $a_2 = \nu(a_{\text{Ge}} - a_{\text{Si}}) + a_{\text{Ge}} = 5.828 \text{ \AA}$ , where  $a_{\text{Ge}} = 5.6575 \text{ \AA}$  is the lattice constant of bulk Ge, and  $\nu = 2\sigma / (1 - \sigma)$ , with  $\sigma \approx 0.273$  the Poisson ratio for Ge. We chose  $a_1 = 5.658 \approx (a_{\text{Si}} + a_2) / 2$ . The Monte Carlo simulation then results in an angular scan as shown in Fig. 1. Corresponding to the previously published experiments<sup>7</sup> a 1.8-MeV beam of  $\text{He}^+$  projectiles incident along a  $\langle 110 \rangle$  axis was assumed and the scan was carried out in a  $\{100\}$  plane. The Si cap thickness was taken as 148 ML. [Here and in the following we define 1 ML as the number of sites on a Si(100) surface,  $6.78 \times 10^{14}$  atoms/cm<sup>2</sup>.] While the Si backscattered yield (triangles), normalized to the random value, from the cap is sym-

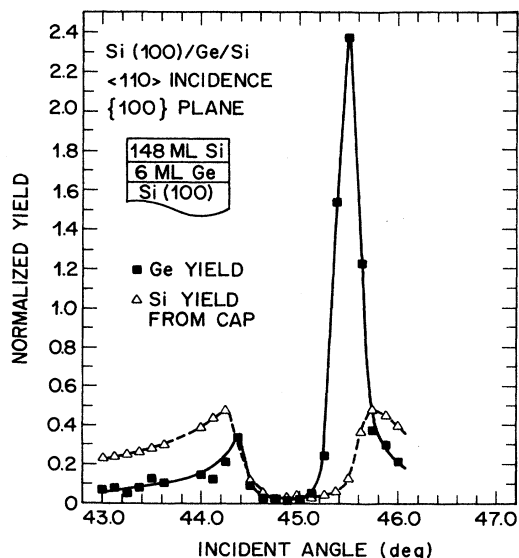


FIG. 1. Simulated angular scan for a structure consisting of 6 ML of Ge and 148 ML of Si grown pseudomorphically on a Si(100) substrate (inset). 1.8-MeV  $\text{He}^+$  projectiles were assumed to be incident around a  $\langle 110 \rangle$  channeling direction. The scan took place in a  $\{100\}$  plane. The normalized yield from the Si cap as well as from the Ge interlayer is shown. The relevant parameters are described in the text.

metric, the yield from the strained Ge interlayer (squares) shows a striking asymmetry similar to the one observed experimentally.<sup>7</sup>

The reason for this asymmetry is immediately obvious when we consider the flux distribution of particles leaving the cap and entering the thin Ge slab. Figure 2 shows the particle flux distribution at the first Si/Ge interface for several different incident angles. The primary beam and the surface [001] normal always lie in the (100) plane. The view in Fig. 2 is into the crystal along the  $[01\bar{1}]$  channeling direction. Each dot represents the position of a projectile right at the interface, projected onto the  $(0\bar{1}1)$  plane. The four crosses represent the equilibrium positions of the four strings visible in the shown area of the crystal projected on the  $(0\bar{1}1)$  plane. The smearing of each string due to thermal motion is shown schematically by the circles centered on a cross, with the radius of each circle equaling the rms displacement for a Si atom. Also shown are the positions of the Ge atoms in a 6-ML-thick layer with respect to a string axis for  $a_1 = 5.658 \text{ \AA}$  and  $a_2 = 5.828 \text{ \AA}$ , represented by their corresponding rms-displacement circles. In all the panels of Fig. 2 the probability of finding a projectile in a particular area  $\delta A$  is directly proportional to the areal density of the dots times  $\delta A$ . For incidence of the primary beam along the  $[01\bar{1}]$  channeling direction ( $\theta = 45.00^\circ$ ) the channeling effect is very obvious: The flux is pushed away from the strings and correspondingly the Si backscattered yield is very low (Fig. 1, triangles). Since the distance to the middle of the channels, where the flux peaks under these conditions, is much larger than the distance that the Ge atoms protrude into the channel, the Ge yield is also low (Fig. 1, squares). For  $\theta = 45.50^\circ$  [Fig. 2(b)] and  $\theta = 44.50^\circ$  [Fig. 2(c)] the high-flux regions shift away from the center of the channels, peaking much closer to the strings. The Si backscattered yield increases significantly (Fig. 1), but is still symmetric in angle with respect to the channel axis because the flux distribution has the same kind of symmetry. Note that the Si strings overlap with the flux distribution only due to the thermal motion. However, the displacements of the Ge atoms not only lead to a direct overlap with the flux at  $\theta = 45.50^\circ$ , giving rise to the corresponding large peak in yield at that angle, but also lead to less overlap at  $\theta = 44.50^\circ$  with the corresponding lowering of the shoulder for that angle. For angles even further away from the channeling direction [Fig. 2(d),  $\theta = 43.00^\circ$ ] the bridgelike structures in the flux distribution break up and the regime of planar channeling is entered. Due to the orientation of the scan plane the overlap between flux and Ge atoms is small, no matter what their displacements, and the Ge yield drops to low values.

The above discussion of the flux distribution suggest that most of the information about the structure at the interface is carried in the asymmetry of the Ge angular scan. We consequently define an asymmetry parameter  $\gamma = Y_{\text{max}}^{\theta > 45^\circ} / Y_{\text{max}}^{\theta < 45^\circ}$ , with  $Y_{\text{max}}^{\theta > 45^\circ}$  the maximum of the backscattered yield for angles larger than  $45.00^\circ$  and  $Y_{\text{max}}^{\theta < 45^\circ}$  the maximum in the yield for angles smaller than  $45.00^\circ$ . We investigate the feasibility and limits of that approach in the following. Figure 3(a) shows  $\gamma$  as a func-

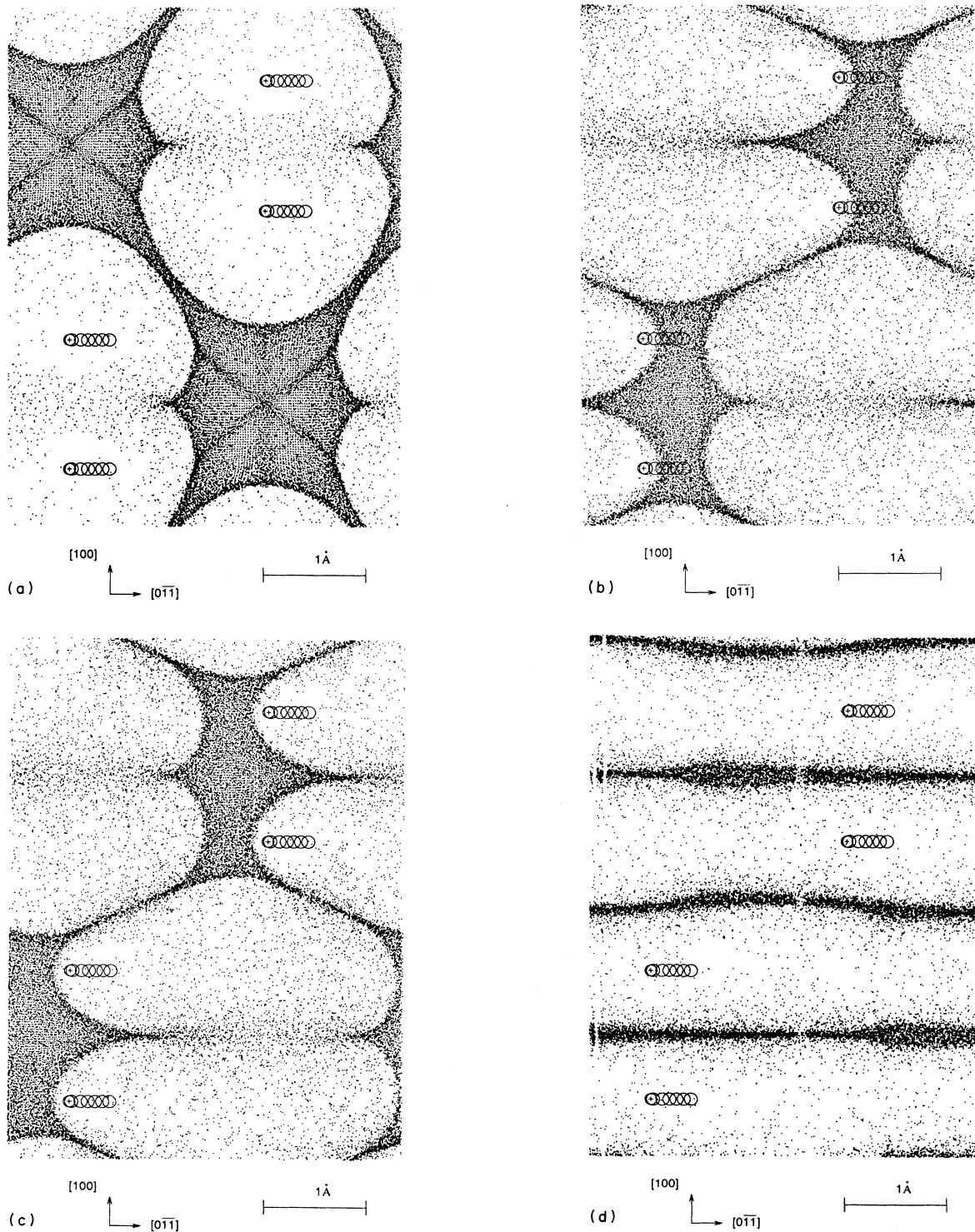


FIG. 2. Flux distributions for the case described in Fig. 1 at the interface between Si cap and Ge interlayer for different angles between the sample normal and the primary beam. Each dot represents the penetration point at that interface of a particle trajectory, projected onto the  $(0\bar{1}1)$  plane. The areal density of dots in a particular area  $\delta A$  multiplied by  $\delta A$  is directly proportional to the probability of finding a projectile in that area. The view is along the  $[0\bar{1}1]$  channel; crystallographic directions are indicated together with a scale marker at the bottom. The crosses in each figure represent the projections of the relevant Si atomic strings. The radius of each circle centered on a string axis represents the root-mean-square (rms) displacement experienced by the Si atoms in the string. Also shown are the positions of the Ge atoms in layers 1–6 of the Ge interlayer with respect to a string, based on  $a_1 = 5.658 \text{ \AA}$  and  $a_2 = 5.828 \text{ \AA}$  and represented by their corresponding rms-displacement circles. Each panel shows a particular incident angle: (a)  $45.000^\circ$ ; (b)  $45.50^\circ$ ; (c)  $44.50^\circ$ ; (d)  $43.00^\circ$ .

tion of  $a_1$  and  $a_2$  for 6 ML of Ge capped with 148 ML of Si. Figure 3(b) is an analogous plot for a 2-ML-thick Ge layer. The shaded areas in each figure are the experimentally determined asymmetries including their estimated error bands.<sup>7</sup> It is obvious that in each case several combinations of  $a_1$  and  $a_2$  give satisfactory agreement with

the experimental data. Indeed, one expects the asymmetry to depend on a combination of  $a_1$  and  $a_2$  since only the total distance  $x_1^{(n)}$  of a Ge atom from a string matters. Here  $n=1,2,\dots$  denotes the Ge layer number, counting from the first Ge/Si interface. Then,

$$x_1^{(n)} = \frac{1}{4\sqrt{2}}[a_1 + (n-1)a_2 - na_{\text{Si}}]. \quad (1)$$

Nevertheless, it is possible to exclude a significant number of possible values for  $a_1$  and  $a_2$ . If we make the further assumption that  $a_1$  and  $a_2$  are the same in both 6- and 2-ML structures, the choice can be further narrowed

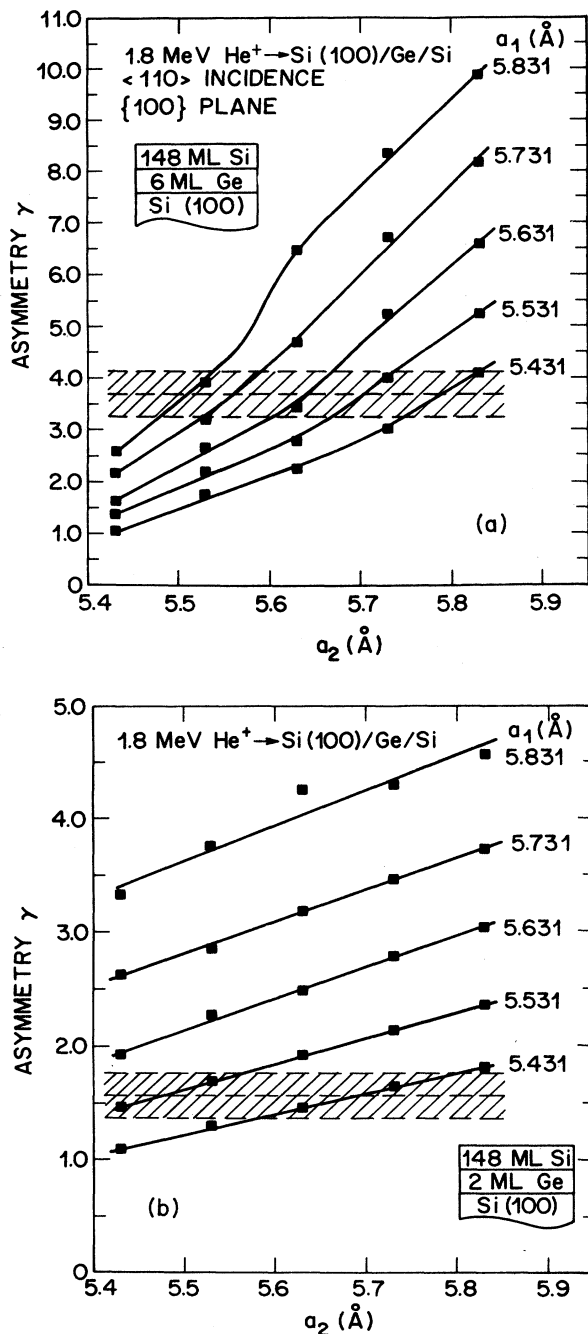


FIG. 3. Asymmetry parameter  $\gamma$  for a structure consisting of (a) 6 ML and (b) 2 ML of Ge on Si(100) substrate capped with 148 ML of Si (inset), as a function of the structural parameters  $a_1$  and  $a_2$ . The shaded areas in each figure are the experimentally determined asymmetries and their estimated error bands.<sup>7</sup> The solid lines have been drawn to guide the eye.

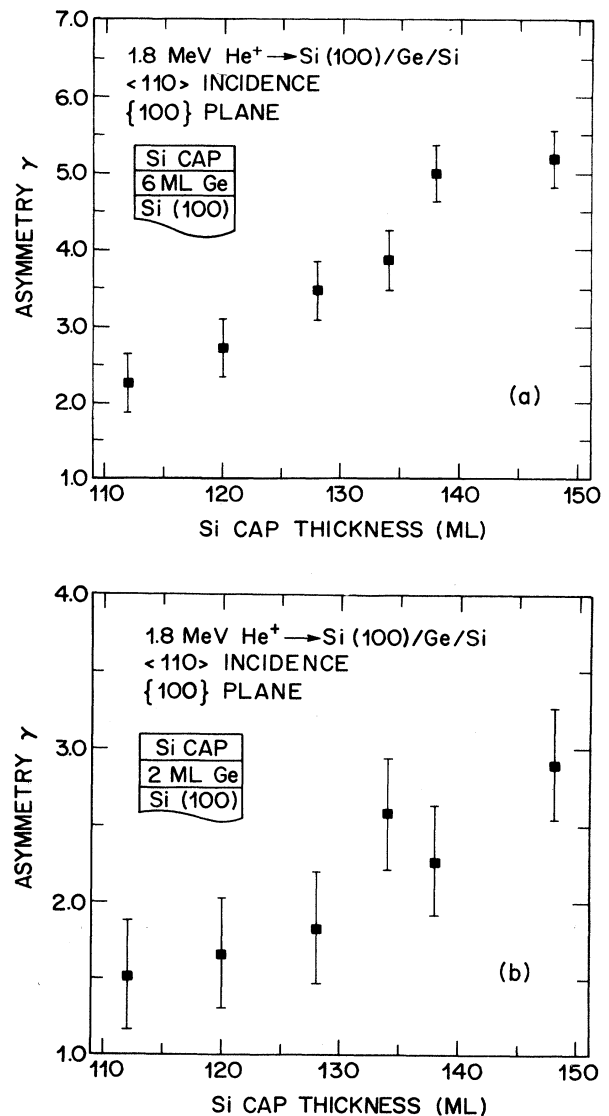


FIG. 4. Asymmetry parameter  $\gamma$  for a structure consisting of (a) 6 ML and (b) 2 ML of Ge on Si(100) as a function of cap thickness. Values of  $a_1 = 5.658$  Å and  $a_2 = 5.828$  Å were used. The error bars have been estimated by determining the asymmetry at a given cap thickness several times, each time using a statistically independent Monte Carlo simulation.

down to  $a_1 \approx 5.43 \text{ \AA}$  and  $5.73 < a_2 < 5.83$ . The value for  $a_2$  agrees very well with the expectation based on the theory of elasticity and a value of  $\sigma = 0.273$  for the Poisson ratio of Ge. The value for  $a_1$ , proportional to the Si—Ge bond length at the first Si/Ge interface, is indistinguishable from the Si bulk lattice constant, and lower than what one might have expected.

#### IV. DISCUSSION

In contemplating this result it is important to keep the possible error sources in mind. The simulations make the assumption of a perfect structure, i.e., sharp interfaces, laminar layers, no steps, and no defects of any kind. Simple terraces of sufficient size ( $> 100 \text{ \AA}$ ) would not influence the channeling experiment, nor has any evidence for island growth been found by electron microscopy;<sup>6</sup> the defect level is below that observable by channeling.<sup>6</sup> However, the assumption of sharp interfaces might not be entirely justified. Recent Raman experiments<sup>20</sup> indicate the possibility of intermixing on the one monolayer scale. Since  $a_1$  basically measures the lattice constant at the interface between Si and Ge, it would be very sensitive to this small amount of grading, leading to a possible reduction in its value from that for a sharp interface. The simulations also assume that the thickness of the crystalline part of the Si cap is precisely known. This is an important parameter, as illustrated in Fig. 4, where the asymmetry is plotted as a function of Si overlayer thickness for a 6-ML Ge layer (a) and for a 2-ML layer (b), and with  $a_1 = 5.658 \text{ \AA}$  and  $a_2 = 5.828 \text{ \AA}$ . Significant changes occur in  $\gamma$  for relatively small changes in cap thickness. While the amount of Si deposited on the Ge interlayer is nominally known to about 1%,<sup>21</sup> the channeling experiment is done after transfer of the sample through air. The growth of the natural oxide, which will invariably occur, will decrease the thickness of the crystalline cap in an uncontrolled way. For a nominal cap thickness of 148 ML, a reduction in thickness of the crystalline part of the cap by 3.4%, corresponding to a native oxide of  $\approx 20 \text{ \AA}$ , would reduce the asymmetry by 0.75 and would lead to an overestimation of  $a_1$  when the simulations are compared with the experimental data.

The simulations also do not take into account the finite spread of the incident beam in the experiment (the beam divergence is  $\approx 0.06^\circ$ ). Including this spread would smear out the sharp peaks in the calculated angular scans, again leading to a lowering of the simulated asymmetry value. Finally, the flux peaking effect is a very sharp function of the incident angle. The full width at half maximum of the peak at angles larger than  $45^\circ$  can become as small as  $0.25^\circ$ , requiring a spacing of the data points of at most  $0.25^\circ/2$ . The spacing of points in the experiment described in Ref. 7 is  $0.2^\circ$  and might be insufficient to completely resolve a peak.

#### V. SUMMARY

In conclusion, we have investigated nonequilibrium phenomena in the channeling of 1.8-MeV  $\text{He}^+$  in ultrathin, (2–6)-ML-thick Ge films on Si(100) substrates, capped with a thin crystalline film of Si. Using Monte Carlo techniques we find that the experimentally observed large asymmetry in the angular scans is directly related to the strain in the Ge films and can be used as a sensitive measure of that strain. Other film parameters, such as possible changes of vibrational amplitudes due to strain, the structural perfection of the interface, or possible grading and/or alloying at the interface, all modify the displacements of the atoms from strings and the flux distribution of the incident projectiles. They can, in principle, be included in the structure search. However, in order to extend the search in this fashion, the parameters of the channeling experiment itself, such as the thickness of the crystalline cap, the beam divergence, and the angular spacing of the data points, have to be well controlled and judiciously chosen. The asymmetry is sensitive to these parameters and the features in the angular scans are extremely sharp functions of angle. This limits any further analysis of the Si/Ge/Si system at present by the angular resolution of the available experimental data.

#### ACKNOWLEDGMENTS

It is a pleasure to acknowledge useful discussions with L. C. Feldman, J. Bevk, and G. J. Fisanick.

<sup>1</sup>L. C. Feldman, J. W. Mayer, and S. T. Picraux, *Materials Analysis by Ion Channeling* (Academic, New York, 1982); H.-J. Gossmann and L. C. Feldman, *Mater. Res. Bull.* **12**, 26 (1987); **12**, 30 (1987).  
<sup>2</sup>J. Lindhard, K. Dan. Vidensk. Selsk. Mat.-Fys. Medd. **34**, No. 1 (1965).  
<sup>3</sup>F. Bøgh, *Radiat. Eff.* **12**, 13 (1972); F. Abel, G. Amsel, M. Bruneaux, and C. Chen, *Phys. Lett.* **42A**, 165 (1972); E. N. Kaufmann, *Phys. Rev. B* **17**, 1024 (1978).  
<sup>4</sup>J. U. Andersen, N. G. Chechenin, and Z. Z. Hua, *Appl. Phys. Lett.* **39**, 758 (1981).  
<sup>5</sup>W. K. Chu, W. R. Allen, J. A. Ellison, and S. T. Picraux, *Nucl. Instrum. Methods B* **13**, 39 (1986).  
<sup>6</sup>J. Bevk, J. P. Mannaerts, A. Ourmazd, L. C. Feldman, and B.

A. Davidson, *Appl. Phys. Lett.* **49**, 286 (1986).  
<sup>7</sup>L. C. Feldman, J. Bevk, B. A. Davidson, H.-J. Gossmann, and J. P. Mannaerts, *Phys. Rev. Lett.* **59**, 664 (1987).  
<sup>8</sup>M. T. Robinson and D. S. Oen, *Phys. Rev.* **132**, 2385 (1963).  
<sup>9</sup>D. V. Morgan and D. van Vliet, *Can. J. Phys.* **46**, 503 (1968).  
<sup>10</sup>J. H. Barrett, *Phys. Rev. B* **3**, 1527 (1971).  
<sup>11</sup>C. Varelas and J. Biersack, *Nucl. Instrum. Methods* **79**, 213 (1970).  
<sup>12</sup>C. Lehmann and G. Leibfried, *Z. Phys.* **172**, 465 (1963); C. Varelas and R. Sizmann, *Radiat. Eff.* **25**, 163 (1975); H.-J. Gossmann, Ph.D. thesis, State University of New York at Albany, 1984.  
<sup>13</sup>L. H. Thomas, *Proc. Cambridge Philos. Soc.* **23**, 542 (1926); E. Fermi, *Z. Phys.* **48**, 73 (1928); G. Molière, *Z. Naturforsch.*

- 2a, 133 (1946).
- <sup>14</sup>O. H. Nielsen, University of Aarhus Internal Report, 1979 (unpublished).
- <sup>15</sup>R. S. Nelson, M. W. Thompson, and H. Montgomery, *Philos. Mag.* **7**, 1385 (1962); D. P. Jackson, B. M. Powell, and G. Dolling, *Phys. Lett.* **51A**, 87 (1975).
- <sup>16</sup>D. P. Jackson and J. H. Barrett, *Phys. Lett.* **71A**, 359 (1979).
- <sup>17</sup>K. Kinoshita, T. Narusawa, and W. M. Gibson, *Surf. Sci.* **110**, 369 (1981).
- <sup>18</sup>O. H. Nielsen and W. Weber, *J. Phys. C* **13**, 2449 (1980).
- <sup>19</sup>D. J. Martin, *Acta Crystallogr. Sect. A* **37**, 851 (1981).
- <sup>20</sup>J. Menéndez, A. Pinczuk, J. Bevk, and J. P. Mannaerts, *J. Vac. Sci. Technol. B* **6**, 1306 (1988).
- <sup>21</sup>J. Bevk, B. A. Davidson, L. C. Feldman, H.-J. Gossmann, J. P. Mannaerts, S. Nakahara, and A. Ourmazd, *J. Vac. Sci. Technol. B* **5**, 1147 (1987).